Structural Safety 74 (2018) 1–13

Contents lists available at ScienceDirect

Structural Safety

journal homepage: www.elsevier.com/locate/strusafe

Performance-based engineering and multi-criteria decision analysis for sustainable and resilient building design

Khalid M. Mosalam[a,*], Umberto Alibrandi[b], Hyerin Lee[c], Jaume Armengou[d]

[a] The Pacific Earthquake Engineering Research (PEER) Center, 723 Davis Hall, Department of Civil and Environmental Engineering, University of California, Berkeley, CA 94720-1710, USA

[b] Berkeley Education Alliance for Research in Singapore (BEARS), CREATE Tower, 1 Create Way, #11-02, Singapore 138062, Singapore

[c] Department of Disaster Prevention Engineering, Chungbuk National University, 1 Chungdae-ro, Seowon-gu, Cheongju 28644, South Korea

[d] Academic Organization and International Relations, School of Architecture, Universitat Internacional de Catalunya, 22 Immaculada St., 08021 Barcelona, Spain

ARTICLE INFO

Keywords:
Building holistic design
Decision making
Energy-efficiency
First-order reliability method
Multi-criteria decision analysis
Performance-based engineering

ABSTRACT

In this paper, an integrated approach for a holistic (involving notions of resiliency and sustainability) building design is presented to select the optimal design alternative based on multiple conflicting criteria using the multi-attribute utility theory (MAUT). A probabilistic formulation of MAUT is proposed, where the distributions of the uncertain parameters are determined by a performance-based engineering (PBE) approach. Here PBE is used to evaluate the building energy efficiency and sustainability in addition to structural safety. In the proposed framework, different design alternatives of a building are ranked based on the generalized expected utility, which is able to include the most adopted probabilistic decision models, like the expected utility and the cumulative prospect theory. The distributions of the utilities are obtained from the first-order reliability method to provide (*i*) good tradeoff between accuracy and efficiency, and (*ii*) rational decision making by evaluating the most critical realizations of the consequences of each alternative through the design point. The application of the proposed approach to a building shows that design for resilience may imply design for sustainability and that green buildings (alone) may be not resilient in the face of extreme events.

1. Introduction

Sustainable development of the urban communities is strictly related to the "disaster risk management" whose aim is the reduction of the "disaster risk." Following [1], it is noted that "natural disaster" do not exist, only natural hazards. Thus, the disaster risk reduction may be achieved by improving the practices of design and construction of the buildings or through wise environmental management. The resilience is defined as the "ability to prepare for anticipated hazards, to adapt to changing conditions, to withstand and recover fast from disruptive events induced by hazards" [2,3]. The sustainability is the "development that meets the needs of the present without compromising the ability of future generations to meet their own needs" [4]. Sustainable development requires a holistic view involving jointly the main pillars of sustainability and resilience (e.g. economy, ecology, society, technical and organizational) and being able to provide the real-time management of the infrastructural systems, incorporating human systems, energy systems, environmental systems, and urban systems. This can be obtained through an integrated design process, involving the different lifecycle phases: design, operation and maintenance, up to demolition or renovation. The task is challenging because there are several sources of uncertainty, the number of stakeholders is high, and the lifecycle of a building is long. Thus, it is crucial to develop an integrated methodical framework as a decision support tool for the optimal decision amongst alternatives subjected to uncertainty and incomplete information.

In a decision-making process, the first step is the choice of suitable performances $G_1,G_2,...,G_n$ expressed in terms of the direct interest of various stakeholders to define the global performance of the system. Together with the performances, the decision maker explores several design alternatives and/or actions through the building lifecycle. Subsequently, making use of the decision making system, the optimal alternative may be determined with general consensus from the stakeholders. The optimal choice takes into account multiple conflicting criteria by making use of the multi-attribute utility theory (MAUT) [5]. An important challenge of MAUT for sustainable design stems from the different sources of uncertainty, giving rise to a problem of decision under uncertainty or under risk. Thus, the objective of this paper is to

* Corresponding author.
E-mail addresses: mosalam@berkeley.edu (K.M. Mosalam), umbertoalibrandi@bears-berkeley.sg (U. Alibrandi), hyerinlee@chungbuk.ac.kr (H. Lee), jarmengou@uic.es (J. Armengou).

https://doi.org/10.1016/j.strusafe.2018.03.005
Received 8 September 2016; Received in revised form 22 March 2018; Accepted 23 March 2018

develop a full probabilistic formulation of MAUT. The main task is modeling the probability distribution of the chosen performances in real-world engineering systems. We adopt the performance-based engineering (PBE) methodology, which is extensively used for evaluating system performance measures meaningful to various stakeholders, e.g. monetary losses, downtime, and casualties [6]. PBE approach links, in a natural way, the building design to the desired performances. For this reason, from PBE emerges principles of resilient design and sustainable design as well. Thus, PBE represents a simple and effective tool for holistic building design.

The second step in a decision-making process is the determination of the optimal probability distribution of the performances for different design options. The most popular approach in civil engineering is the equivalent cost analysis where all the performances are converted into a monetary measure through suitable conversion factors; in such case, the alternatives are compared in terms of the minimum expected cost [7]. However, research suggests that the risk cannot be entirely monetized [8]. In the utility theory, it is recognized that subjective factors should be taken into account in the risk evaluation, and this is accomplished through the utility function, which measures the desirability of the consequences. In such case the optimal alternative gives the maximum expected utility [9]. It is well recognized that the expected utility is not able to provide an accurate description of the observed behavior of the decision makers [10,11]. Some improvements have been proposed, like the cumulative prospect theory [12–14], which integrates the risk perception inside the formulation of the utility function, and it recognizes the subjective evaluation of the probability of occurrence of rare events. The main difficulty is the definition of a suitable probability weighting function measuring perception of the likelihood of the events. Recently, some researchers have proposed to rank the alternatives through the adoption of risk measures (e.g. expected values, quantiles, or superquantiles) applied to the performances [15,16].

In this paper, it is proposed to rank the alternatives through a variant of the expected utility, called generalized expected utility (GEU), able to incorporate most existing decision models (e.g. expected utility, cumulative prospect theory, risk measures) as particular cases. It is also proposed to model the risk aversion in the GEU by applying the superquantile to the utilities U.

A rational decision making can be obtained through a good understanding of the consequences [17]. This is accomplished by determining the distributions of the utilitiese through the first-order reliability method (FORM), which gives a good tradeoff between accuracy and efficiency. Moreover, the knowledge of the design point provides significant realizations of the consequences corresponding to chosen alternatives/actions. The FORM results can effectively guide the decision maker to make a rational choice of the optimal design.

The decision-making process is dynamic in the sense that the optimal decision changes when new information is available. Such dynamic behavior is effectively represented through Bayesian analysis, here modeled through the adoption of Bayesian Networks [18]. The formulation can be used for updating the uncertain input variables, but also the subjective utilities expressing the degree of preference of the decision maker and of the different stakeholders involved in the design process [19,20]. In cases where the scarcity of data makes the probabilistic analysis problematic, the optimal decision may be explored through sensitivity analysis of the decision outcomes to the various input parameters.

The proposed framework represents a powerful tool for an extended multi-objective system of management and design under uncertainty. After describing the main features of the framework, it is applied to a hypothetical office building located in California. The example shows the main strengths of the proposed approach and its capabilities for pursuing sustainable and resilient building design.

2. Multi-criteria decision making under uncertainty

Multi-criteria decision-making problems involve optimal design in the presence of multiple design criteria, typically conflicting each other. In this paper, we adopt the widely used multi-attribute utility theory (MAUT) [5] whose aim is the selection of the "best" design alternative from a pool of m preselected alternatives $a^{(1)},a^{(2)},\cdots,a^{(m)}$, explicitly known in the beginning of the solution process. The evaluation of the optimal solution is based upon the preferences of the decision maker with respect to a set of performances, or decision criteria. From a mathematical point of view, the performance of a system can be described through a set of functions $G_r = g_r[\boldsymbol{x},\boldsymbol{v}(\boldsymbol{x})]$, $r = 1,2,\cdots$ where $\boldsymbol{x} = \{x_1 \quad x_2 \quad \cdots \quad x_q\}$ collects all the "design variables" containing the control variable values representing the set of preselected alternatives, i.e. $\boldsymbol{x}^{(k)} \equiv a^{(k)}$. The vector $\boldsymbol{v}(\boldsymbol{x}) = \{\boldsymbol{v_B} \quad \boldsymbol{v_D}(\boldsymbol{x})\}$ collects all the uncertain parameters appearing in the decision-making problem where $\boldsymbol{v_B}$ collects the *basic random variables*, which are the parameters that cannot be controlled by the decision maker, e.g. hazards or environmental conditions and $\boldsymbol{v_D}(\boldsymbol{x})$ collects the *derived parameters* that are affected by the design variables, e.g. uncertain responses of the system.

2.1. Selection and definition of criteria and design alternatives

In a decision-making model, the Requirements are the most general standpoints, e.g. Functional, Social, Environmental, and Economical [21,22], which may be unfolded in several Criteria or Attributes (e.g. lifecycle cost), where each criterion may involve several Performance Indicators, e.g. energy expenditure and economic losses, see Table 1. Typically, there are several criteria to consider and generally some of them may be inevitably conflicting. The first step in the decision-making problem is to identify from the criteria a set of n performances $G_1,G_2,...,G_n$ collected in the vector $\boldsymbol{G}$. The next step is to define a finite set of m design alternatives, i.e. $\boldsymbol{a} = \{a^{(1)} \quad a^{(2)} \quad ...a^{(m)}\}$. The performance of the system depends on all indicators $G_1,G_2,...,G_n$ and it is defined through the multi-attribute function $G_s[\boldsymbol{G}(\boldsymbol{x})]$, while the performance of the i-th alternative $a^{(i)}$ reads as $G_s^{(i)} = G_s[\boldsymbol{G}(\boldsymbol{x}^{(i)})] \equiv G_s[\boldsymbol{G}^{(i)}]$.

Table 1
Requirements, criteria and indicators for a building.

Requirement	Criteria	No.	Performance Indicator
Functional	Quality perception	1	User
		2	Visitor
	Adaptability to changes	3	Modularity
Economic	Construction cost	4	Direct Cost
		5	Deviation
	Lifecycle cost	6	Utilization
		7	Maintenance
		8	Losses
Social	Integration of science	9	New patents
	Work for local companies	10	Turnover
	Annoyance of construction	11	Dust
		12	Noise
		13	Street occupation
	Safety of construction	14	Risk of casualties
Environmental	Construction	15	Water consumption
		16	CO_2 emission
		17	Energy consumption
		18	Raw materials
		19	Solid waste
	Integration in environment	20	Visual
	Utilization	21	Noise, dust, smell
		22	Energy consumption
		23	CO_2 emission
	Reintegration	24	Solid waste

2.2. MAUT

In MAUT, each alternative receives a score through the definition of suitable overall utility functions defined in terms of the chosen performances. To rank the alternatives, it is necessary to define a measure of the alternatives themselves. Generally, as discussed above, the performances have different units of measure and they may be hardly quantified into a single composite measure. This is resolved in MAUT through the utility function, which converts the values of the performances to scores representing the *degree of preference* of the decision maker within the decision model. For each design alternative, an utility function $u^{(i)} = u(G_1^{(i)},G_2^{(i)},...,G_n^{(i)})$ is defined such that the most and least beneficial options have utilities $u_{max}^{(i)} = 1$ and $u_{min}^{(i)} = 0$, respectively. Other options have utility scores between these limits, which are higher when the performance of a given alternative is better. The utility function $u(\boldsymbol{G})$ is expressed as a combination of single attribute utility functions $u_j(G_j)$ of only one performance where the relative importance is defined by weights w_j, $0 \leqslant w_j \leqslant 1$, $\sum_{j=1}^{n} w_j = 1$, of the different performances. Several methods for assigning the weights are discussed in [23]. A simple model of aggregating the attributes is the following *linear model*.

$$u(G_1,G_2,...,G_n) = \sum_{j=1}^{n} w_j u_j(G_j) \tag{1}$$

The additive rule in Eq. (1) is generally valid if the consequences, expressed in terms of degree of preference of the decision maker, of the interaction between indicators G_j are negligible.

The shape of the utility functions may contain information about the risk attitude of the decision maker [24,5]. A simple single-attribute utility function is *linear* as follows,

$$u_j(g_j) = \begin{cases} 1.0 & g_j \leqslant g_{j,min} \\ (g_{j,max}-g_j)/(g_{j,max}-g_{j,min}) & g_{j,min} < g_j < g_{j,max} \\ 0.0 & g_j \geqslant g_{j,max} \end{cases} \tag{2}$$

where $g_{j,min}$ and $g_{j,max}$ are respectively the most and least beneficial values of the indicator, which is representative of a risk-neutral attitude. If the values of the performances were known with certainty, the optimal decision corresponds to the maximum utility, i.e. $u^{(opt)} = u(g_1^{(opt)},g_2^{(opt)},...,g_n^{(opt)}) = max\{u^{(1)},u^{(2)},...,u^{(m)}\}$. However, in real-world applications, the indicators G_j are uncertain. In such cases, the alternatives are ranked through the expected utility *EU*, expressed as follows,

$$EU^{(i)} = \int u(\boldsymbol{g}) dF_{\boldsymbol{G}}^{(i)}(\boldsymbol{g}) = \int u(\boldsymbol{g}) f_{\boldsymbol{G}}^{(i)}(\boldsymbol{g}) d\boldsymbol{g} \tag{3}$$

while the optimal alternative maximizes the *EU*. In Eq. (3) and in the rest of the paper, f indicates the probability density function (PDF), F is the cumulative distribution function (CDF) and $P = 1-F$ is the probability of exceedance (POE).

2.3. Utility theory

The dominant idea in the theory of choice under uncertainty is the definition of a functional $\mathscr{V}(\cdot)$ applied to the performance G, such that if $\mathscr{V}(G^{(1)}) \geqslant \mathscr{V}(G^{(2)})$, then the alternative $G^{(1)}$ is preferred to the alternative $G^{(2)}$. The expected utility *EU*, formulated in Eq. (3), represents a class of functionals state-independent "linear in the probabilities." By assuming that the performance is the economic cost c and that the decision maker is risk-neutral, see Eq. (2), the maximum *EU* is equivalent to the minimum expected cost expressed as follows,

$$\max_{c^{(i)}} EU \equiv \min_{c^{(i)}} E[C] = \min_{c^{(i)}} \int P_C^{(i)}(c)\, dc \tag{4}$$

The last equation comes from an integration by parts of the expected value of the cost [25] and it is attributed to the fact that the area under the P_C curve, is used in current PBE for comparing design decisions [26].

Differently from expected cost, the *EU* may also incorporate the behavioral concept of risk aversion of the decision maker, modeled through the utility function $u(c)$ and expressing the attitude towards the outcomes. From the other side, criticism of the axiomatic foundation of *EU* are well-documented from the early days of the utility theory, especially with reference to the *independence axiom*, which addresses the so-called "rationality" in the *EU* theory [10,27,17]. A major feature of the violations of the *EU* is the apparent overweighting of low probability events with extreme consequences. This issue is of great importance for decision making in civil engineering. A popular solution is represented from the cumulative prospect theory [12]. It has been already applied in civil engineering for modeling the risk aversion for seismic risk mitigation of building structures [28,13,14]. It appears to have the potential to describe the risk-averse choices of the decision makers. However, its practical implementation in terms of elicitation of the utility function and of the risk perception is not an easy task.

3. Generalized expected utility

It is noted that the utility function of the i^{th} alternative $U^{(i)} = u(\boldsymbol{G}^{(i)})$ is a random variable since $\boldsymbol{G}^{(i)}$ is a vector of random variables, see Eq. (1). It depends on the corresponding joint PDF $f_{\boldsymbol{G}}^{(i)} = f_{\boldsymbol{G}}^{(i)}(\boldsymbol{g})$ of the indicators $\boldsymbol{G}^{(i)}$, which can be determined from the PBE approach. Since $U^{(i)}$ is a random variable, it is completely defined by its CDF, which can be evaluated through the structural reliability theory by introducing a limit state function $G_s(\xi,\boldsymbol{G}^{(i)}) = u(\boldsymbol{G}^{(i)})-\xi$, where $F_U^{(i)}(\xi) = Prob[G_s(\xi,\boldsymbol{G}^{(i)}) \leqslant 0]$, i.e.

$$F_U^{(i)}(\xi) = Prob[u(\boldsymbol{G}^{(i)}) \leqslant \xi] = \int_{\{G_s(\xi,\boldsymbol{G}^{(i)}) \leqslant 0\}} f_{\boldsymbol{G}}^{(i)}(\boldsymbol{g})\, d\boldsymbol{g} \tag{5}$$

The general framework of probabilistic MAUT is illustrated in Fig. 1. In this figure, we consider two different alternatives $a^{(1)}$ and $a^{(2)}$ with respect to two different performance indicators G_1 and G_2. For each indicator we define the utility functions $u_1(g_1)$ and $u_2(g_2)$, while the multi-attribute utility function is $u(g_1,g_2) = w_1u_1(g_1) + w_2u_2(g_2)$. The performances G_1 and G_2 are random variables whose joint distributions for the two alternatives are $f_{G_1G_2}^{(1)}(g_1,g_2)$ and $f_{G_1G_2}^{(2)}(g_1,g_2)$, shown in the bottom left and right corners of the figure. Correspondingly, two utilities are defined, $U^{(1)} = u(G_1^{(1)},G_2^{(1)})$ and $U^{(2)} = u(G_1^{(2)},G_2^{(2)})$.

The knowledge of the CDF of $U^{(i)}$ fully defines the utility of the i^{th} alternative, since its POE $P_U^{(i)}(\xi) = Prob[u(\boldsymbol{G}^{(i)}) \geqslant \xi]$ is equal to the complementary CDF, i.e. $P_U^{(i)}(\xi) = 1-F_U^{(i)}(\xi)$, while the PDF may be determined as $f_U^{(i)}(\xi) = \partial F_U^{(i)}/\partial\xi$. To rank the alternatives, one variant of the cumulative prospect theory is proposed herein, called generalized expected utility (*GEU*) and expressed as follows,

$$GEU^{(i)} = \int u^{(i)} d[h\{F_U^{(i)}\}] \tag{6}$$

It is decision model embodying a fundamental distinction between attitudes to the outcomes, measured by $u(\cdot)$, and attitudes to the probabilities, distorted through $h(F_U)$. It is easy to see that if the probabilities are not distorted, i.e. $h(F_U) \equiv F_U$, then Eq. (6) gives the expected value of $U^{(i)}$ and the *GEU* is coincident with *EU* as shown below,

$$GEU^{(i)} \equiv E[U^{(i)}] = \int u^{(i)} dF_U^{(i)}(u) = \int u(\boldsymbol{c}) dF_{\boldsymbol{C}}^{(i)}(\boldsymbol{c}) \equiv EU^{(i)} \tag{7}$$

A challenge in *GEU* is represented from the elicitation of the utility function. In the literature, some authors think that a rational decision maker should be risk neutral by considering complete consequence models. In [17], it is conjectured that the risk-aversion intrinsic to nonlinear utility functions can be explained by the non-inclusion of "follow-up" consequences. In other words, they assume that if perfect information were available, then a rational decision maker would be risk neutral. Suppose that the losses are given by the annual loss L, and to reduce the risks, the decision maker decides to buy an insurance cover, so that the annual cost c according to [29] becomes,

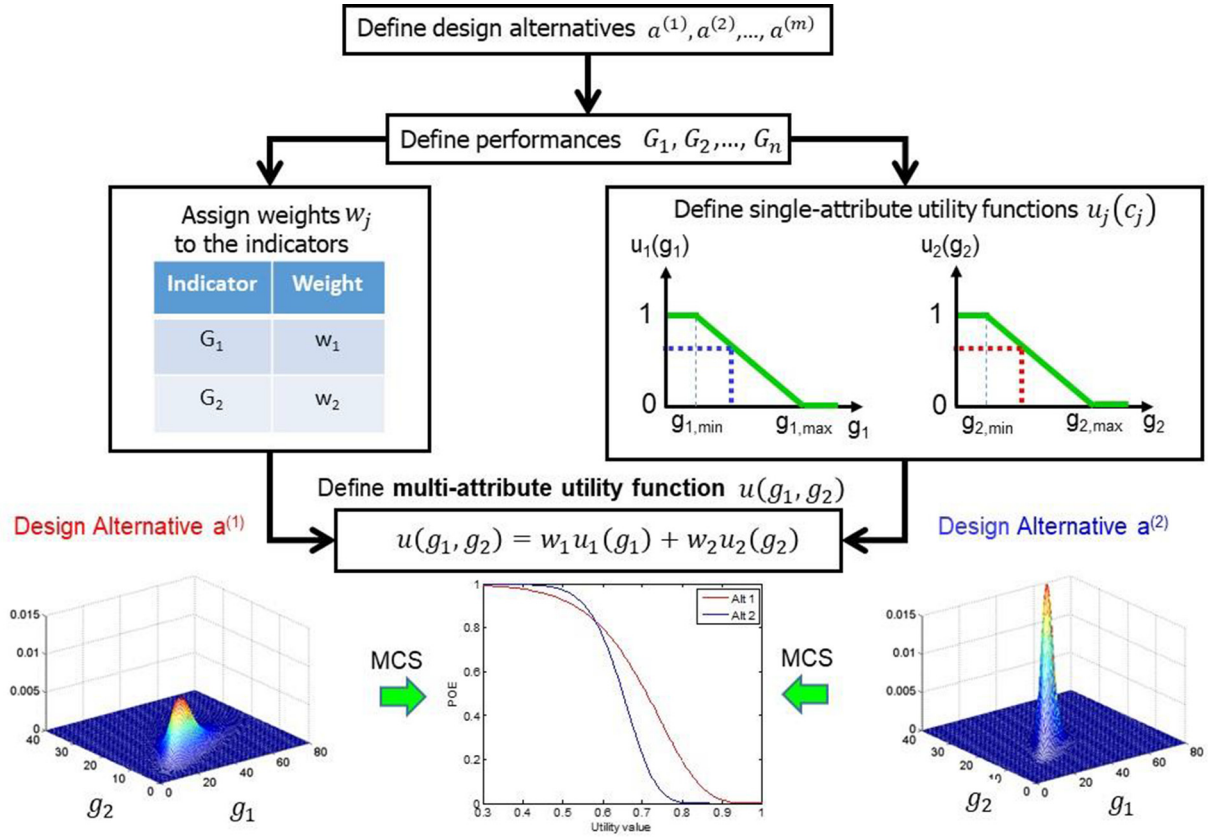

Fig. 1. Schematic of the probabilistic MAUT.

$$c = (L - L_{cov}) + c_i = L + (c_i - L_{cov}) = L + \varphi(L) \tag{8}$$

where c_i is the cost of acquiring the protection (insurance premium and deductible) while L_{cov} is the maximum monetary value that an insurance company will pay the owner of a property following an occurring hazard. It is noted that the function φ depends on L, since c_i and L_{cov} depend on the probability of the incurred damage cost. In such cases a decision maker may wish to apply a risk-averse utility function $u_{RA}(L)$ to the losses L (without including the follow-up contributions $\varphi(L)$ of the insurance) or alternatively to keep a risk-neutral attitude by including them, i.e. $u_{lin}[L + \varphi(L)]$. Of course, the two formulations are equivalent from a mathematical point of view, i.e. $E[u_{RA}(L)] = E[u_{lin}(L + \varphi(L))]$, but only the second one is representative of risk-consistent decision making. Although the *GEU* is broadly general, in this paper, the adoption of linear utility functions with complete models of the consequences is followed. In this manner, the utility function expresses the preference ordering of the decision maker, while his/her risk-aversion is described only through the function $h(F_U)$, which defines the attitude toward the probability ("increased uncertainty hurts" [30]). Several models for $h(F_U)$ can be adopted and here a model is proposed as follows,

$$h(F_U) = \begin{cases} \frac{1}{\alpha} F_U & 0 \leqslant F_U \leqslant \alpha \\ 0 & F_U > \alpha \end{cases} \tag{9}$$

which gives rise to the following formulation

$$GEU(\alpha) = E[U | 0 \leqslant u \leqslant \xi] = \frac{\int_0^{\xi} u f_U \, du}{\int_0^{\xi} f_U \, du} = \frac{1}{\alpha} \int_0^{\alpha} u \, dF_U \tag{10}$$

where $\xi \equiv q_U(\alpha) = F_U^{-1}(\alpha)$, with $0 \leqslant \xi \leqslant 1$, is the α-quantile of U while $GEU(\alpha)$ is its α-superquantile $\overline{q}_U(\alpha)$ (or conditional quantile) [15,16]. The superquantile is an average of quantiles for probability levels $0 < \alpha' < \alpha$, see Fig. 2, and it has some attractive mathematical properties, like coherency and regularity. In figure it is chosen $\alpha = 0.20$, which means that the (risk-averse) choice of the decision maker is driven by the choice of the 20% worst events. It is noted that for, $\alpha = 1$, $GEU(1) = \overline{U}$, and $GEU \equiv EU$, while the left tail of $f_U(u)$, corresponding to extreme events with low utility, is defined for low values of α, which provide risk-averse decisions. In other words, with Eq. (9), the *GEU* provides the *conditional expected utility*, while a risk-averse decision is obtained by considering only the events providing the lowest utilities. Thus, the $GEU(\alpha)$, for $\alpha < 1$, can be interpreted as the assessment of a risk-neutral decision maker that is uncertain about the validity of the distribution of $U = u(\boldsymbol{G})$, see also [16]. Thus, the alternatives can be ranked through the *EU* by setting $\alpha = 1$. However, if uncertainty about the suitability of the adopted distributions arises or if there is particular concern for the potentially undesired consequences of unlikely events, superquantiles with values $\alpha < 1$ may be chosen. The suitable choice of α can be made through sensitivity analyses, as discussed below.

4. Evaluation of the distribution of the utility functions

The utility $U^{(i)} = u(\boldsymbol{G}^{(i)})$ is a function of random variables, which also makes it a random variable itself. Our focus is on a *multi-criteria decision making*, such that $U^{(i)}$ takes into account several joint criteria, typically conflicting, and whose consequences (direct and indirect) can go beyond economic issues. However, in Eq. (1), the contributions of several criteria are combined into a single random variable, while for an informed decision, it would be useful to know the values of the most critical realization of the performances, for a chosen degree of risk-aversion. This is obtained by applying the FORM to $U^{(i)}$, as described below. The evaluation of the distribution of the utilities, Eq. (5), can be performed using structural reliability theory.

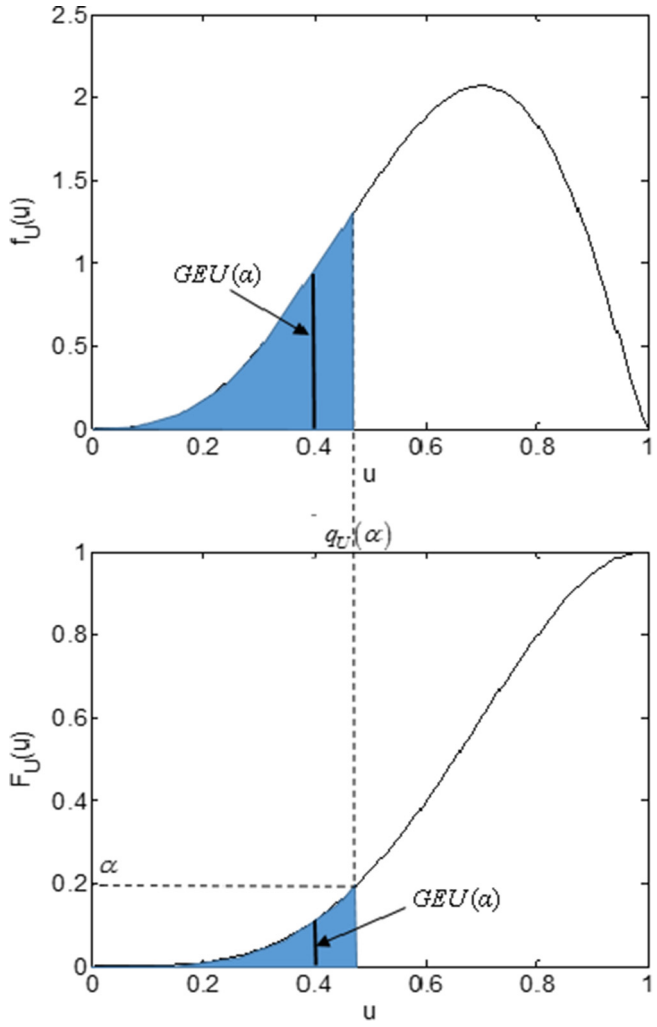

Fig. 2. Schematic of the superquantile.

4.1. FORM

A good tradeoff between accuracy and efficiency is provided by the FORM. After probabilistic transformation towards the standard normal space $\boldsymbol{u}$, Eq. (5) becomes,

$$F_U^{(i)}(\xi) = Prob[U^{(i)}(\boldsymbol{u}) \leqslant \xi] = \int_{\{g_s^{(i)}(\xi,\boldsymbol{u})\leqslant 0\}} \varphi_n(\boldsymbol{u}) d\boldsymbol{u} \tag{11}$$

where $\varphi_n(\boldsymbol{u})$ is an n variate PDF of the normal standard distribution, while $g_s^{(i)}(\xi,\boldsymbol{u}) = U^{(i)}(\boldsymbol{u}) - \xi$ is the multi-attribute limit state function in the normal standard space corresponding to the i^{th} alternative. The design point $\boldsymbol{u}_i^*(\xi)$ is the most likely realization of the random variables giving rise to the event $[g_s^{(i)}(\xi,\boldsymbol{u}) \leqslant 0] \equiv [U^{(i)}(\boldsymbol{u}) \leqslant \xi]$, i.e. the point closest to the origin of the standard normal space of the limit state surface $g_s^{(i)}(\xi,\boldsymbol{u}) = 0$ and obtained as the solution of an optimization problem,

$$\boldsymbol{u}_i^*(\xi) = argmin\{\|\boldsymbol{u}\|: g_s^{(i)}(\xi,\boldsymbol{u}) = 0\} \tag{12}$$

The reliability index is defined as the distance to the design point from the origin of the standard normal space $\beta_i(\xi) = \|\boldsymbol{u}_i^*(\xi)\|$. Thus, FORM gives an approximation of the distribution $F_U^{(i)}(\xi) = \Phi[-\beta_i(\xi)]$, where Φ is the CDF of the normal standard distribution, to that defined by Eq. (11) and it is accurate enough for most cases of practical interest. If this is not the case, the recently proposed secant hyperplane method [31,32] can be used.

4.2. The role of the design point for PBE-MAUT

Typically, a decision maker desires to choose the best alternative having some information about the consequences of the choices. This may be obtained easily by noting that

$$\beta_i(\xi) = \Phi^{-1}[1-F_U^{(i)}(\xi)] = \Phi^{-1}(1-\alpha) \tag{13}$$

Through an algorithm of inverse reliability [33] for a chosen $\beta = \beta_0$, corresponding to probability $\alpha_0 = \Phi(-\beta_0)$ of the distribution of the utility function, the threshold $\xi_0^{(i)}$ of $U^{(i)}$ is determined such that $\beta_i(\xi_0^{(i)}) = \beta_0$. Once $\xi_0^{(i)}$ is evaluated, the corresponding limit state function $g_s(\xi_0^{(i)},\boldsymbol{u}) = U^{(i)}(\boldsymbol{u}) - \xi_0^{(i)}$ is defined, and the design point $\boldsymbol{u}_{0i}^* = \boldsymbol{u}_i^*(\xi_0^{(i)})$ together with its mapping in the original space $\boldsymbol{G}_{0i}^* = \boldsymbol{G}_i^*(\xi_0^{(i)})$ are determined. Thus, each alternative is defined by a single deterministic value $\boldsymbol{G}_{0i}^*$ for a chosen quantile. The alternatives can also be ranked through a deterministic MAUT by applying Eq. (1) to the design points, i.e. $U^{(i)} = U(\boldsymbol{G}_{0i}^*)$.

The application of MAUT to the design points corresponding to different quantiles allows not only to choose the best design alternative, but also to give information about the most critical realization of the indicators for different degrees of risk. In this manner, the decision maker can select, consciously, the best alternative, taking into account all consequences of all scenarios, including the worst ones.

The optimal alternative is measured through the *GEU*, and the risk perception described through the superquantile of U. Application of FORM to a sequence of thresholds allows to determine, with reduced computational effort, the quantities of interest $GEU^{(i)}$. Moreover, following the procedure described above, it is possible to determine the most critical realizations $\boldsymbol{G}_{\alpha i}^* = \boldsymbol{G}_i^*(GEU^{(i)})$ corresponding to the chosen superquantiles. In this manner, the decision maker can have a clear understanding of the utilities of the different alternatives together with the corresponding consequences for different values of quantiles and superquantiles, the latter including also the expected utility.

5. Joint distribution of the uncertain parameters

A key point in the determination of the distributions of the utility functions is represented by evaluating the joint PDF $f_{\boldsymbol{G}}^{(i)}(\boldsymbol{g})$ of the indicators, Eq. (5). It is underlined that especially the tails of the utility functions are sensitive to the distributions of the input parameters $G_1,G_2,...,G_n$, which therefore have to be modeled as accurately as possible, given the available information.

5.1. PBE approach

The Pacific Earthquake Engineering Research (PEER) Center developed a robust PBE methodology focused on earthquake engineering (PBEE), which is based on explicit determination of system performance measures meaningful to various stakeholders such as monetary losses, downtime, and casualties based on probabilistic assessment [34,6]. The PEER PBEE methodology consists of four successive analyses: hazard, structural, damage, and loss. The methodology focuses on the probabilistic calculation of meaningful system performance measures considering the involved uncertainties in an integrated manner. PBE can be one of the solutions to estimate the performance corresponding to each chosen performance, not only structural losses, but also other criteria such as construction and maintenance costs, CO_2 emission during the construction and operation phases, and energy expenditure *EE*. This is the approach followed in this paper. For the sake of clarity, consider as an example some criteria corresponding to the seismic risk. In this case, the following PBE variables can be adopted: (*i*) Intensity measure *IM* of the hazard, e.g. the peak ground acceleration (*PGA*) or the pseudo-spectral acceleration of the structure at its natural period of vibration; (*ii*) Engineering demand parameter $EDP(\boldsymbol{x})$, e.g. maximum peak inter-story drift ratio along the building height or the peak roof acceleration;

(*iii*) Damage measure $DM(\boldsymbol{x})$ denoting damage levels for structural and non-structural components; (*iv*) performance $G(\boldsymbol{x})$ (called decision variable DV in the PEER PBEE framework). The performance can be the economic loss $L(\boldsymbol{x})$ due to seismic hazard in a given period, or the corresponding functionality loss of the building. Therefore, we have

$$P[EDP_i] = \sum_m P[EDP_i|IM_m]p(IM_m) \tag{14}$$

$$P[DM_k] = \sum_i P[DM_k|EDP_i]p(EDP_i) \tag{15}$$

$$P[L_n] = \sum_k P[L_n|DM_k]p(DM_k) + \sum_m P[L_n|C]P[C|IM_m]p(IM_m) \tag{16}$$

where $P[X_i]$ is the POE of the i -th value of the random quantity X_i, $P[X_i|\ Y_j]$ is the conditional POE of X_i given Y_j, $p(X_i)$ is the probability of occurrence of X_i. With respect to the losses L_n, it is likely to observe global collapse at higher intensity level, and in PEER-PBEE, this collapse is treated separately from the case when no collapse occurs. Thus, in Eq. (16), $P[L_n|\ C]$ is the POE of L given the collapse, and $P[C|\ IM_m]$ is the probability of collapse given the i-th value of IM. In the case of economic loss, the dependence on the price fluctuation factors can also be considered. In the case of determining the POE of a specific sustainability performance, the following variables can be used: (*i*) Climate variable CV, (*ii*) Energy consumption $EC(\boldsymbol{x})$, (*iii*) performance $G(\boldsymbol{x})$, e.g. CO_2 emissions and energy expenditures EE,

$$P[EC_k] = \sum_i P[EC_k|\ CV_m]p(CV_m) \tag{17}$$

$$P[CO_2] = \sum_k P[CO_2|\ EC_k]p(EC_k) \tag{18}$$

$$P[EE] = \sum_k P[EE|\ EC_k]p(EC_k) \tag{19}$$

It is noted that the two different types of performances (hazard-related and sustainability-related) can be interconnected, because the CO_2 can be generated by post-hazard repairs [35], i.e.

$$P[CO_2] = \sum_k P[CO_2|\ DM_k]p(DM_k) \tag{20}$$

Accordingly, the evaluation of the distribution of the performance CO_2 may require the evaluation of the conditional distributions $P[CO_2|\ EC_k]$ and $P[CO_2|\ DM_k]$.

The adoption of the PBE methodology [34] has several advantages: (*i*) it is based on the total probability theorem, which requires elementary knowledge of probabilistic concepts and thus easily adopted and interpreted in practice, (*ii*) it is already applied for the evaluation of the safety of structures subjected to seismic hazard by practicing engineers, making the extension to different hazards and other performances straightforward, and (*iii*) the different stages of the analysis can be performed by separate groups of multi-disciplinary research team.

Following [18], it is natural to formulate the proposed approach for sustainable and resilient building design inside the framework of the Bayesian networks, which are graphical probabilistic models that facilitate efficient representation of the dependence among random variables [36]. The Bayesian networks have a transparent modeling, and they can be adopted by users with limited background in probabilistic or reliability analyses. Fig. 3(a) represents the classical PBE framework applied to seismic risk formulated in terms of a Bayesian network. Note that the derived variables as well as the performances are expressed in terms of $\boldsymbol{x}$, to denote their dependence on the design variables, represented by the alternatives. In Fig. 3(b), the holistic framework is represented, including issues of sustainability and resilience. Here, three performances have been chosen: $G_1 \equiv L$ (losses), $G_2 \equiv CO_2$ emission and $G_3 \equiv EE$ (energy expenditure), with the utility functions expressed as $U = U(G_1,G_2,G_3)$. The links from DM (damage measure) to L indicate that the distribution of L is conditioned on DM (see Eq. (16)). In a similar manner, it is seen that the distribution of CO_2 is conditioned on DM (see Eq. (20)) and energy consumption EC (see Eq. (18)). The Bayesian networks are based on the Bayes' rule and the Bayesian inference, such that the network is updated in real-time when new information is acquired, e.g. through network of sensors or new experimental tests. The Bayesian networks can also be used to update the utility functions $u_j(G_j)$ or the knowledge of the weights w_j. For further details about this topic, the interested reader is referred to [18].

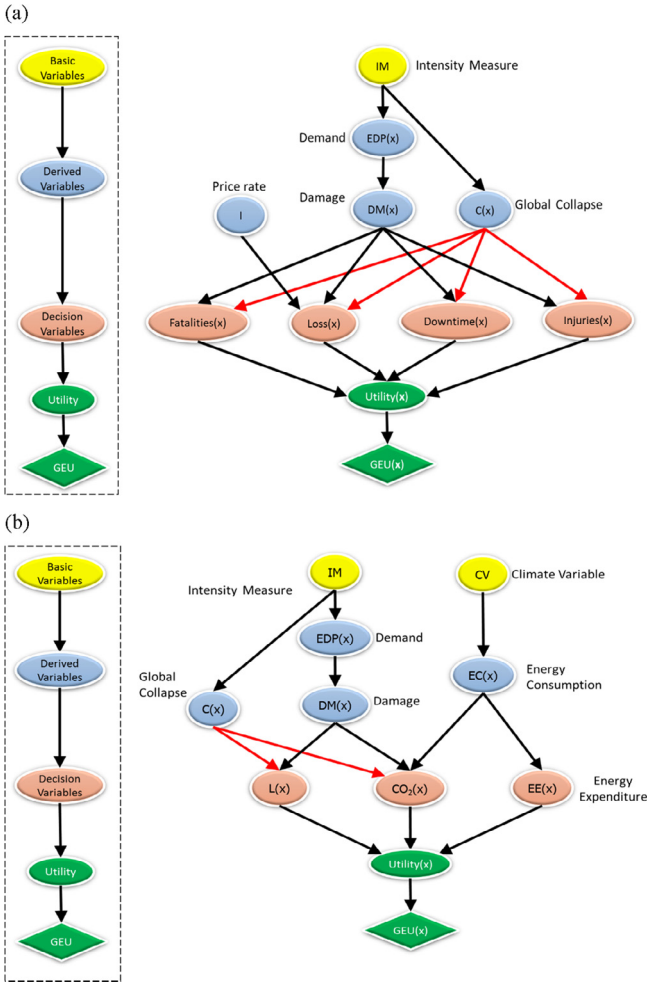

Fig. 3. Schematic of PBE-MAUT through Bayesian networks. (a) Performance-based earthquake engineering, (b) Holistic design.

5.2. Probability distributions

If only a small sample of data is available, the marginal distributions can be modeled using known parametric distribution, e.g. Normal, Lognormal, or Weibull, with parameters determined through the "method of the moments" or the "method of maximum likelihood." A statistical test to accept or reject the probability model is usually adopted. However, for an assigned physical quantity, in presence of samples of small size, it is often difficult to statistically justify a specific single distribution. An effective tool for this purpose is represented by the "method of the maximum entropy" [37,38] giving the least biased distribution with respect to the available information. A kernel density estimation based on the maximum entropy principle, which adopts generalized moments, is recently proposed in [39]. The method, called kernel density maximum entropy method, may be considered an effective approach for evaluating the optimal distributions of the performances $G_1,G_2,...,G_n$ [40] and can also elicit the utility functions in terms of preferences of the decision maker.

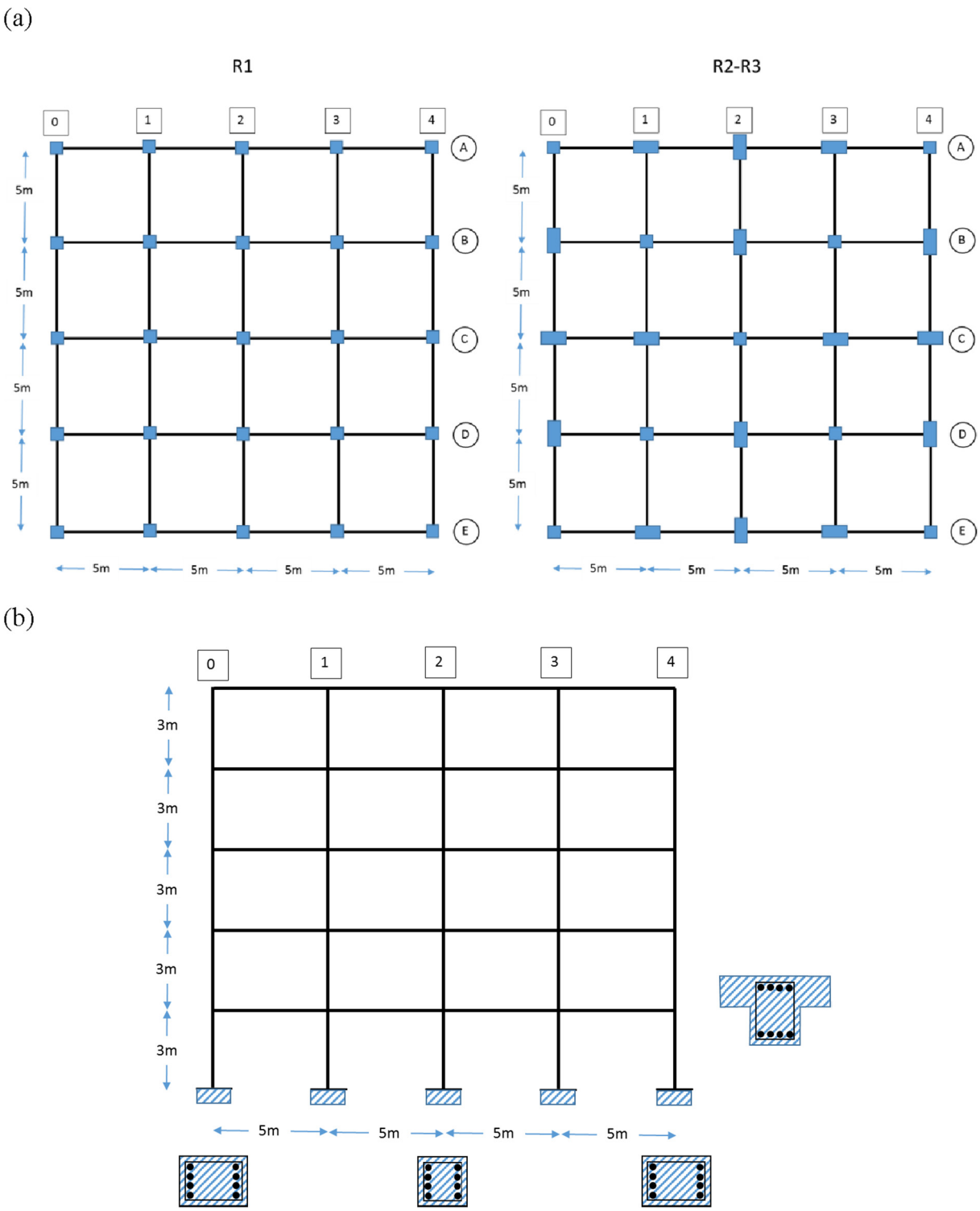

Fig. 4. Plan and elevation view of the example building. (a) Plan view, (b) Elevation view, frame C.

In some cases, the scarcity of data may prevent the definition of a reliable probability distribution, in terms of PDF and/or its parameters. In such cases, suitable distributions based on engineering judgment and/or expert opinion may be adopted [41]. If new information becomes available, it will be used to update the probability distributions of the uncertainties through Bayesian updating, as discussed above and in [18]. In cases where the lack of available data and statistics to determine the input parameters can limit the usefulness of the method, the sensitivity of the decision outcomes to the various input parameters may then be analyzed.

6. Application example

A hypothetical four-bay five-story reinforced concrete (RC) office building is considered. The building has plan dimensions of 20 × 20 m, with floor-to-floor height of 3 m. The floors and the roof are 200 mm thick RC slabs supported by columns whose spacing is 5 m. Fig. 4 shows plan and elevation views of this building. Given the fully symmetric

configuration of the building, a two-dimensional model is adopted. Following [42], the vertical design loads are: (*i*) self-weight, (*ii*) 958 Pa for superimposed dead load given by electrical, mechanical, plumbing, and floor and ceiling fixtures, and (*iii*) 2400 Pa for live loads of a typical occupancy of an office building.

6.1. Resilient design – seismic risk

In this subsection, the seismic risk losses developed inside the framework of PBE will be discussed, see [6]. The corresponding formulation in terms of Bayesian networks is shown in Fig. 3(a). The beam sections are 300 × 500 mm with 8 reinforcing bars of 16 mm diameter, providing 1.07% longitudinal reinforcement ratio. Three different designs are considered as alternatives: (*i*) *R1*, where the columns are 300 × 300 mm with 8 reinforcing bars of 14 mm diameter (1.37%), (*ii*) *R2*, where the columns are 300 × 500 mm with 8 reinforcing bars of 16 mm diameter (1.07%), (*iii*) *R3*, where the columns are 300 × 700 mm with 8 reinforcing bar of 20 mm diameter (1.20%).

The lifecycle cost $L(t_n)$ represents the total cost incurred by the building during the lifecycle [43,29], i.e.

$$L(t_n,\boldsymbol{x}) = CC(\boldsymbol{x}) + \sum_{k=1}^{n} C_F(t_k,\boldsymbol{x}) = CC(\boldsymbol{x}) + LCC(\boldsymbol{x}) \tag{21}$$

where $\boldsymbol{x}$ collects the design parameters, t_n is the lifespan typically measured in years, $CC(\boldsymbol{x})$ is the initial cost, $C_F(t_k,\boldsymbol{x})$ is the failure cost at year t_k, while $LCC(\boldsymbol{x})$ is the lifecycle repair cost. Typically, when the design is more conservative, the initial cost $CC(\boldsymbol{x})$ increases, while the failure cost $C_F(t_k,\boldsymbol{x})$ decreases. The initial cost $CC(\boldsymbol{x})$ is usually assumed deterministic, and it includes the cost of the material in the respective material manufacturing, material transportation, and on-site construction phases. The lifecycle failure cost is expressed as

$$C_F(t_k,\boldsymbol{x}) = C_S(t_k,\boldsymbol{x}) + C_{NS}(t_k,\boldsymbol{x}) = \frac{L_S(\boldsymbol{x})}{(1+\gamma_d)^{t_k}} + \frac{L_{NS}(\boldsymbol{x})}{(1+\gamma_d)^{t_k}} \tag{22}$$

where $C_S(t_k,\boldsymbol{x})$ and $C_{NS}(t_k,\boldsymbol{x})$ are the contributions of repair costs of structural and non-structural components, respectively, $L_S(\boldsymbol{x})$ and $L_{NS}(\boldsymbol{x})$ are the corresponding annual losses under the assumption that each year the existing damages are repaired, while γ_d represents the discounting rate, which may be considered if the decision maker considers less painful future costs which are discounted to the net present value. The repair costs of the structural elements are dependent upon the damage state [35] and include cost of the material in the material manufacturing, material transportation, and on-site construction phases and the debris disposal. For simplicity, in this numerical application, the repair costs of the non-structural components are not considered, i.e. $L_{NS} = 0$.

For the three designs, the construction cost is $CC^{(1)} = 1.6$ "$"$M$, $CC^{(2)} = 2$ "$"$M$ and $CC^{(3)} = 2.6$ "$"$M$, corresponding to a unit cost of 800 "$"/m^2, 1000 "$"/m^2 and 1300 "$"/m^2, respectively. The assumed large difference in the construction costs for the three projects is not to be attributed only to the structural cost, which usually represents about one quarter of the total cost, but from the different design options that can arise during the construction stages of a building. The chosen values of the construction costs are here used to show some salient features of the proposed approach, as described below.

6.1.1. Hazard Analysis

The building is located in Berkeley, CA whose latitude and longitude are respectively 37.877° and −122.264°, the site class is assumed to be *D*, with a shear velocity of 259 m/s in the upper 30 m , i.e. V_{s30}. The *PGA* is chosen as an *IM*. The hazard curve is obtained by using the hazard curve calculator application of OpenSHA [44]. Discrete values of *PGA* between 0.05 *g* and 3 *g* with 0.05 *g* increments are chosen, for a total of 60 *IM* values. Hazard analysis includes also the selection of a suitable number of ground motions (GMs) compatible with the site class and the hazard curve. Here, we choose 81 GMs selected from the PEER next generation attenuation (NGA) project GM database [45] with the following selection criteria for magnitude *M*, distance *R*, and shear wave velocity V_{s30}: $6 \leqslant M \leqslant 7.5$, $0 \leqslant R \leqslant 20$ km, $360 \leqslant V_{s30} \leqslant 760$ m/s.

6.1.2. Structural Analysis

The structural analyses are developed by using the software OpenSees [46]. Beams and columns are modeled using displacement-based beam-column elements, i.e. *dispBeamColumn*, with fiber discretized sections. Core and cover concrete are modeled using *Concrete01;* the compressive strength of the concrete is 35 MPa, the concrete strain values at maximum strength and at crushing strength are 0.2% and 0.5%, respectively. Sufficient shear reinforcement is assumed to be provided to eliminate any shear failure. The reinforcing bars are modeled with *Steel01*, whereas the yield strength of the steel is 420 MPa, the elastic modulus is 200,000 MPa, and the strain hardening ratio is $b = 0.05$. The 81 GMs are scaled for each *IM*, giving a total number of analyses of $81 \times 60 = 4860$. For brevity, this study considers only the maximum peak interstory drift ratio (*MIDR*) as *EDP*. For each value of the *IM*, it is assumed that $P[MIDR|\ IM_m]$ follows a lognormal distribution.

6.1.3. Damage Analysis

The definition of the seismic capacity plays a significant role in the definition of the fragility curves. Because of the lack of data to develop probabilistic capacity models, capacity values are based on HAZUS [47], which classifies buildings in terms of their use (occupancy class) and in terms of their structural system (model building type). The considered building belongs to the building structure C1M (Mid-rise concrete moment frame). As described in HAZUS, 4 damage states are considered: slight (DS1), moderate (DS2), extensive (DS3), and Complete (DS4). These qualitative performance levels can be represented by deterministic interstory drift limits of 0.33%, 0.58% 1.56%, and 4.00% of the story height for DS1, DS2, DS3, and DS4, respectively (mid-code values). These values are treated as median values of a lognormal distribution, while the dispersion value is assumed to be 0.3 [48].

6.1.4. Loss Analysis

The loss functions are derived from [35] assuming that the probability distributions $P[L|\ DM = DS_k]$, $k = 1,2,3,4$ follow lognormal distributions whose median values are 15 "$"/m^2, 83 "$"/m^2, 228 "$"/m^2 and 1434 "$"/m^2 for the 4 damage states with assumed dispersion of 0.3. These values correspond to injecting epoxy resin for slight damage (DS1), patching with shotcrete for moderate damage (DS2), jacketing with RC for extensive damage (DS3), and demolition and reconstruction for complete damage (DS4).

6.1.5. Decision under uncertainty

For the three designs *R1*, *R2* and *R3*, the estimated annual loss [49] is evaluated from Eqs. (14)–(16), by defining the distribution of the annual loss $L_S^{(i)}$, see Eq. (21). The total loss $L^{(i)}$, $i = 1,2,3$ is given by the contributions of the construction cost $CC^{(i)}$ and of the lifecycle repair cost determined by assuming a period $T \equiv t_n = 50$ years, where a discount rate of $\gamma_d = 3\%$ has been adopted, see Eq. (21). The resulting distribution is lognormal obtained by fitting the data of 10,000 simulations and it represents the performance of the decision problem. The three distributions $P_L^{(1)}$, $P_L^{(2)}$ and $P_L^{(3)}$ are represented in Fig. 5. Since $P_L^{(2)} \leqslant P_L^{(3)} \leqslant P_L^{(1)}$ everywhere, it follows that the expected utilities are $EU^{(2)} \geqslant EU^{(3)} \geqslant EU^{(1)}$, see Eq. (4). Under these circumstances, the risk aversion to the outcomes given by $u(g)$ and the risk perception toward the unlikely events do not affect the decision. Of course, this is not always the case, and an example is shown in Section 6.2. When only one economic criterion is adopted, the maximum expected utility is coinciding with the minimum expected cost. The expected costs of the three alternatives are given by the area under the loss curves, and they are $E[C^{(1)}] = 5.43$ "$"$M$, $E[C^{(2)}] = 4.24$ "$"$M$ and $E[C^{(3)}] = 4.70$ "$"$M$, with

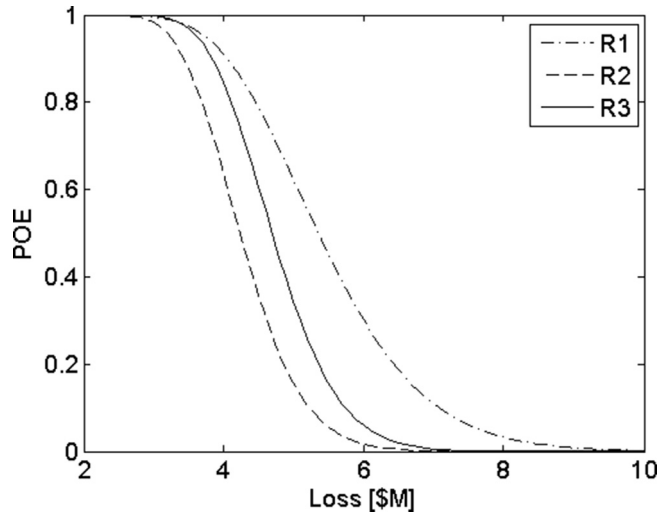

Fig. 5. Distributions of three design alternatives *R1*, *R2*, and *R3* with respect to the performance loss L.

$E[C^{(2)}] \leqslant E[C^{(3)}] \leqslant E[C^{(1)}]$. Following [3], resilience includes both robustness and recovery goals. The robustness goal is an acceptable level of damage immediately following a hazard. The third design *R3* is more robust, so that the lifecycle repair costs are $LCC^{(3)} < LCC^{(2)} < LCC^{(1)}$. However, it is seen that the optimal alternative is given by the design *R2* because it provides a better tradeoff between construction cost and lifecycle cost, i.e. $CC^{(2)} + LCC^{(2)} < CC^{(3)} + LCC^{(3)}$.

6.2. Sustainable design

Sustainability analysis of the building is conducted in this subsection. Here, only economic and environmental requirements are considered. The chosen performances are $G_1 \equiv CO_2$ emission and $G_2 \equiv EE$ as energy expenditure. Two different energy plans are considered as alternative sustainability designs, namely (*i*) Energy plan *P1*, where the energy consumption is supplied 50% by electricity and 50% by natural gas, and (*ii*) Energy plan *P2* where the whole energy is supplied by electricity.

6.2.1. Energy Consumption

Due to lack of data on the thermal insulation properties of the building envelope, and of energy consumption inside the building, average values reported in [50,51] are adopted. The energy intensity for the sum of major fuels is 200.3 kWh/m^2/year in the West-Pacific region, classified as climate zone 4. Since the area of all floors of the considered building is $A_{tot} = 2000$ m^2, its energy consumption *EC* is 400.6 MWh/year. For plan *P1*, where the building is operated by electricity and natural gas, the consumptions of electricity and natural gas in the building are $\overline{EC}_{el}^{(1)} = \overline{EC}_{ng}^{(1)} = 200.3 MWh/year$. For plan *P2*, $\overline{EC}_{el}^{(2)} = 400.6 MWh/year$ is supplied by electricity, while $\overline{EC}_{ng}^{(2)} = 0$. These are assumed to be median values of lognormal distributions, whose dispersion is 0.3.

6.2.2. Sustainability Analysis

From average rates reported in [51] for the West-Pacific region, the CO_2 emission by consuming electricity and natural gas are calculated as $\overline{CO}_{2,el} = 177.4$ kg/MWh and $\overline{CO}_{2,ng} = 228.6$ kg/MWh, respectively. Buildings average prices for electricity and natural gas are assumed to be $\overline{C}_{el} = 104$ "$"/MWh and $\overline{C}_{ng} = 36.2$ "$"/MWh [50], respectively. For the two energy plans *P1* and *P2*, the estimated annual CO_2 emission and annual energy expenditure *DV* are evaluated from Eqs. (18) and (19), respectively, and simulated through Monte Carlo simulation (MCS).

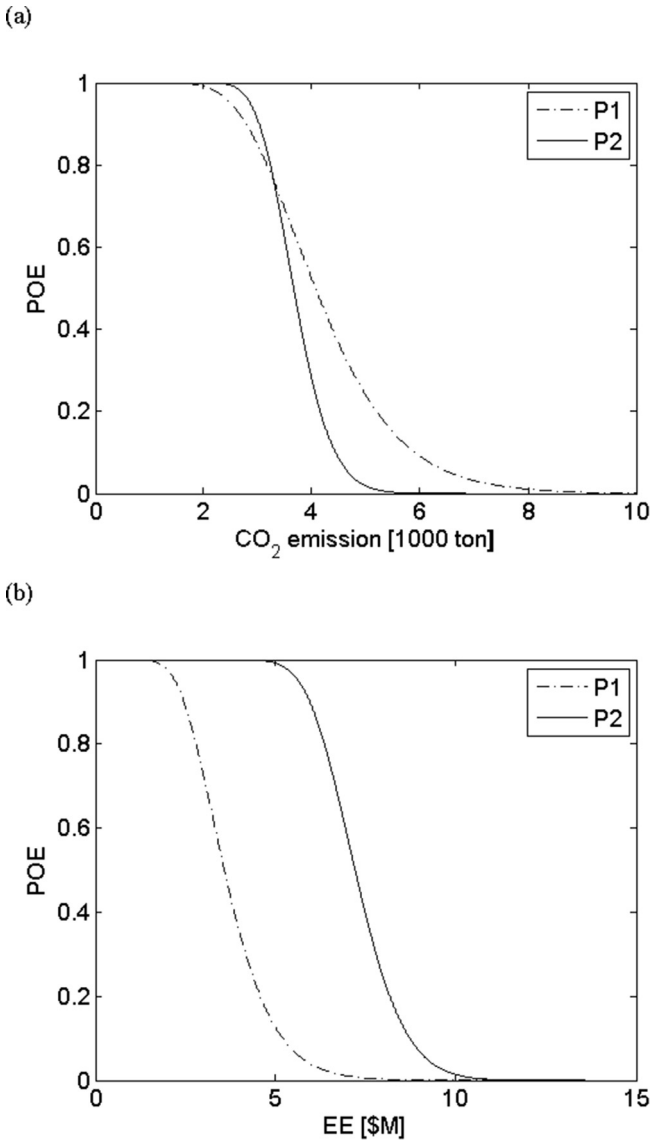

Fig. 6. Marginal distribution of the sustainable performance, (a) $G_1 \equiv CO_2$ emission, (b) $G_2 \equiv EE$ for the two energy plans.

Subsequently, the lifecycle values $EE^{(i)}$ and $CO_2^{(i)}$ $i = 1,2$ during a period $T \equiv t_n = 50$ years are evaluated.

$$EE(t_n,\boldsymbol{x}) = \sum_{k=1}^{n} \left[\frac{EC_{el}(t_k,\boldsymbol{x})\cdot\overline{C}_{el}}{(1+\gamma_{el})^{tk}} + \frac{EC_{ng}(t_k,\boldsymbol{x})\cdot\overline{C}_{ng}}{(1+\gamma_{ng})^{tk}} \right] \tag{23}$$

$$CO_2(t_n,\boldsymbol{x}) = \sum_{k=1}^{n} CO_2(t_k,\boldsymbol{x}) \tag{24}$$

To calculate the net present value of *DV*, based on the estimations from 2010 to 2025, it is assumed that $\gamma_{el} = -0.4\%$ and $\gamma_{ng} = +0.8\%$ per year for electricity (*el*) and natural gas (*ng*). Finally, it is assumed that the same amount of CO_2 is emitted each year; discount rates are not recommended for environmental impacts because of their non-monetary values. A set of 100,000 samples of $CO_2(t_n,\boldsymbol{x})$ and $EE(t_n,\boldsymbol{x})$ is generated, which follows a bivariate lognormal distribution. In Fig. 6, the marginal distributions of CO_2 and *DV* are presented, where it is seen that plan *P1* is more advantageous in terms of economic requisite, while from an environmental point of view, plan *P2* is preferred. The expected values of the performances are $E[CO_2^{(1)}] = 4255.4$ ton and $E[CO_2^{(2)}] = 3716.6$ ton, with $E[CO_2^{(2)}] \leqslant E[CO_2^{(1)}]$, while $E[EE^{(1)}] = 3.75$ "$"$M$ and $E[EE^{(2)}] = 7.30$ "$"$M$ with

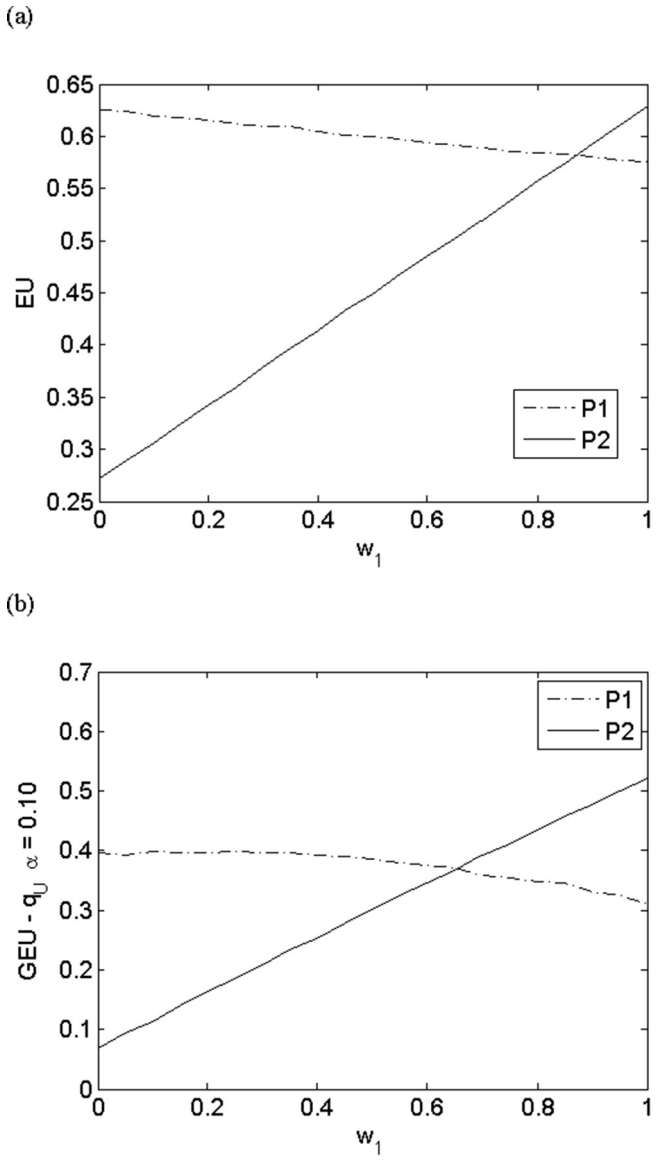

Fig. 7. Sensitivity analysis of the *GEU* in terms of the weight $w_1 \equiv w_{CO_2}$, (a) *EU*, (b) *GEU* measured through superquantile with $\alpha = 0.10$, for the two energy plans.

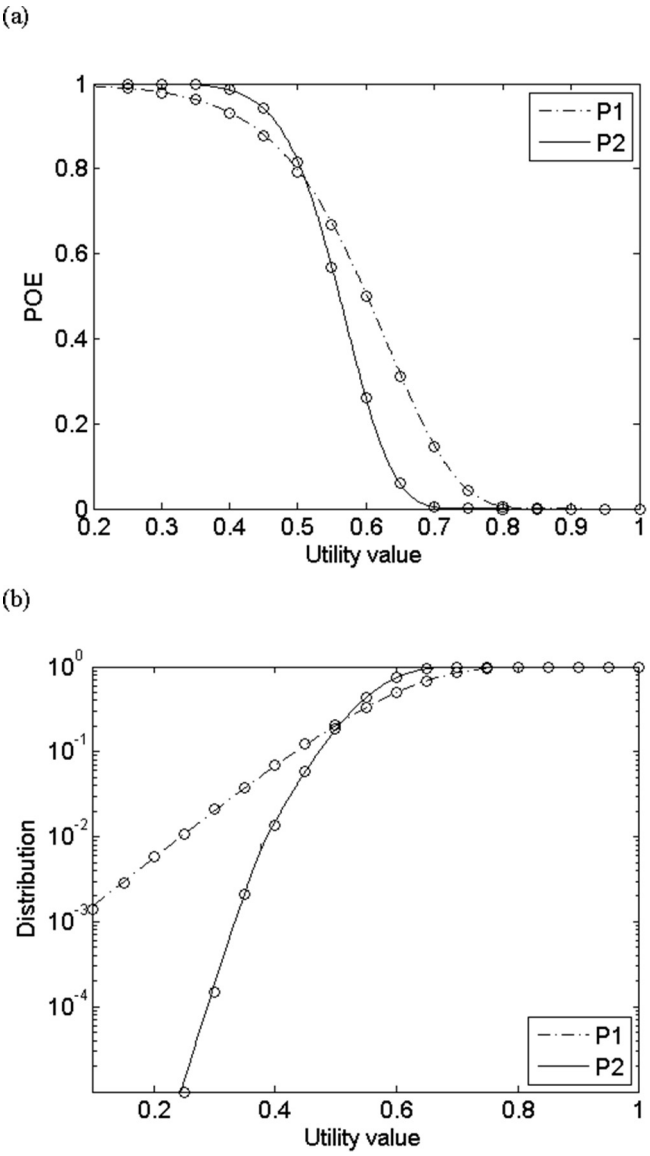

Fig. 8. Distribution of the utility functions corresponding to the two energy plans.

$E[EE^{(1)}] \leqslant E[EE^{(2)}]$. The two performances are conflicting each other. Moreover, differently from the total loss described in Fig. 5, $P^{(1)}_{CO_2} \leqslant P^{(2)}_{CO_2}$ for $CO_2 \leqslant 3550$ tons and $P^{(1)}_{CO_2} \geqslant P^{(2)}_{CO_2}$ for $CO_2 > 3550$ tons. In this case, the risk aversion may affect the optimal choice.

6.2.3. Decision under uncertainty

The possible inhomogeneous units makes the comparisons between alternatives not straightforward. In the utility theory, this is resolved using the utility functions. In the proposed *GEU*, we suggest to adopt a linear model for the utility functions. In Eq. (2), $[c_{j,min};c_{j,max}]$ are assumed [0;10,000] ton and [0;10] "$"$M$ for $G_1 \equiv CO_2$ and $G_2 \equiv EE$, respectively. A challenge in MAUT is the evaluation of the weights, expressing the degree of preference between the criteria. In such case, $w_1 > 0.5$ implies that the decision maker is oriented towards a sustainable design since he/she expresses a degree of preference towards the needs of the future generations (more weight to CO_2, less weight to *DV*). It is of interest to develop a sensitivity analysis of the *EU* and the *GEU* with respect to w_1, see Fig. 7. Here the risk aversion inside the *GEU* is measured through the superquantile with $\alpha = 0.10$. As expected, it is seen that for higher values of w_1, the plan *P2* is preferred, and it can be considered more sustainable.An informed risk-decision requires however an understanding of the consequences of each choice. To this aim, FORM is a powerful tool. Consider for example the case $w_{CO_2} = 0.8$. From Fig. 7, it is seen that for this choice of weights, $EU^{(1)} \geqslant EU^{(2)}$, while $GEU^{(1)} \leqslant GEU^{(2)}$. It is reasonable to think that a risk-averse decision maker can choose *P2* in order to avoid the undesired consequences although unlikely. To show this, FORM is applied to determine the distribution of the utility functions, see Fig. 8. The circle markers indicate the MCS results with 100,000 samples. It is clearly shown that FORM is very accurate in addition to its well-known computational efficiency even in the range of small probabilities. In Fig. 8(b), the CDF of the utilities in semi-logarithmic scale are represented, and it is seen that with plan *P2*, the probability of outcomes giving the lowest utilities is very low. This is explained because $GEU^{(2)} \geqslant GEU^{(1)}$ for $\alpha = 0.10$. In Fig. 9, the sensitivity analysis of *GEU* with respect to α is presented; it is seen that a rational decision maker, maximizing the *EU* (obtained for $\alpha = 1$) should choose plan *P1*, while a risk-averse decision maker can choose plan *P2*.

The choice of a suitable degree of risk-aversion α is supported by the FORM solution. As noted in Eq. (13), $\alpha(\xi) = \Phi[-\beta(\xi)]$, so that for each value of α, it is possible to determine the corresponding design point

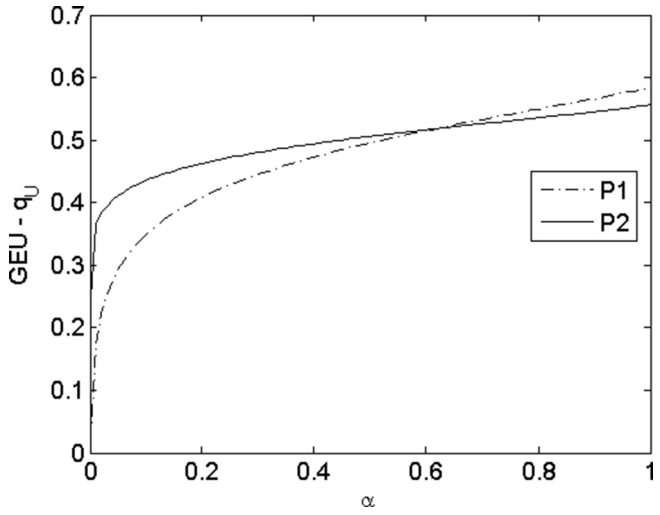

Fig. 9. Sensitivity analysis of *GEU* in terms of α for the two energy plans.

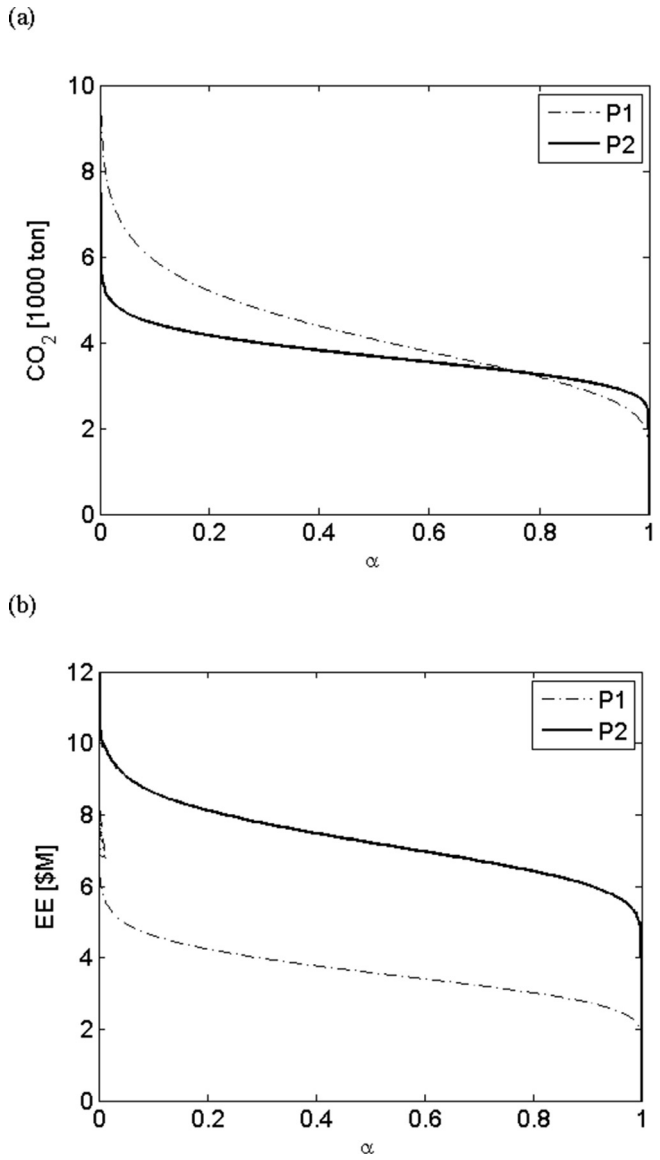

Fig. 10. Sensitivity analyses of the performances in terms of α: (a) CO_2 emission, (b) *EE* for the two energy plans.

$\boldsymbol{u}^*(\xi)$ and its mapping $\boldsymbol{g}^*(\xi)$ in the original space. Fig. 10 shows the most likely realizations of the performances, given by the design points, in terms of α. Thus, the proposed approach, allows to determine not only the optimal decision with chosen degree of risk-averseness, but also the corresponding design values of the criteria. From Fig. 10, it is seen that plan *P1* represents a better choice only if expected event occurs ($\alpha \cong 1$). However, if unlikely event occurs (low values of α), plan *P1* would lead to higher environmental impact. Conversely, plan *P2* allows to keep the environmental safety to reasonable low values in the two considered scenarios (average and unlikely), although it leads to more economic cost.

6.3. Sustainable and resilient design

In this subsection, sustainable and resilient design is considered. The design alternatives considered in the previous subsections are combined, providing six new alternatives: (*i*) *P1-R1*, (*ii*) *P2-R1*, (*iii*) *P1-R2*, (*iv*) *P2-R2*, (*v*) *P1-R3*, and (*vi*) *P2-R3*. The chosen performances of the decision-making problem are CO_2 emission and the economic losses L.

The main difference with respect to the previous analyses is the CO_2 emission because of post-hazard repairs. The conditional probabilities $P[CO_2|\ DM = DS_k]$, $k = 1,2,3,4$ are derived from [35] assuming that they follow lognormal distributions whose median values are 4 kg/m^2, 27 kg/m^2, 171 kg/m^2, and 447 kg/m^2 for the damage states slight, moderate, extensive, and complete, respectively, where the dispersion is assumed to be 0.3. In Fig. 11, the conditional annual probabilities $P[CO_2|\ DM = DS_k,R2]$ and $P[CO_2|\ P2]$ are compared, where $P[CO_2|\ P2]$ is the POE of the CO_2 emission for given energy plan *P2*, while $P[CO_2|\ DM = DS_k,R2]$ are the four POE of the CO_2 emission for the four considered damage states relative to the design *R2*. It is seen that a "green" building characterized by low energy consumption is sustainable only if the probability of occurrence of the damage states DS3 and DS4 are very small. Thus, a sustainable design needs to be resilient towards the extreme events. It is also noted that Fig. 11 shows the conditional probabilities of CO_2 given a damage state, irrespective of the hazard which triggered it. Therefore, resilience toward any type of hazard (wind, flood, blast, degradation, etc.) is a key ingredient for sustainable design.

In Fig. 12, the sensitivity analysis of *EU* and *GEU* with respect to w_1 is presented. In such case, $w_1 > 0.5$ implies that the decision maker is oriented towards a sustainable design since he/she gives more weight to CO_2 and less weight to L. The analysis shows that: (*i*) high resilience guarantees high sustainability (e.g. design *R3* has high values of *EU* and *GEU*), (*ii*) a building cannot be sustainable if it is not resilient (e.g. design *R1* gives the lowest values of *EU* and *GEU*), and (*iii*) the sustainability does not necessarily require a high level of resilience because it is seen that the *GEU* of the alternative *P2-R2* ranks better than *P1-R3* (*P2* is more sustainable than *P1*, while *R3* is more resilient than *R2*.)

7. Concluding remarks

In this paper we have developed a full probabilistic formulation of the multi-attribute utility theory (MAUT) for holistic building design. The uncertainties have been modeled by random variables defined through the performance-based engineering (PBE) approach.

In literature, the optimal decision in seismic risk analysis has often been determined through the minimization of the expected cost or the maximization of the expected utility. Typically, only cost analysis has been considered inside the decision-making process. Here, the procedure has been extended to the integrated framework which takes into account not only the safety of the building, but also environmental responsibility, human comfort (which can be considered in future studies), and energy consumption.

In the decision-making model, a generalized expected utility (*GEU*) has been proposed to rank the alternatives. It is a variant of the known

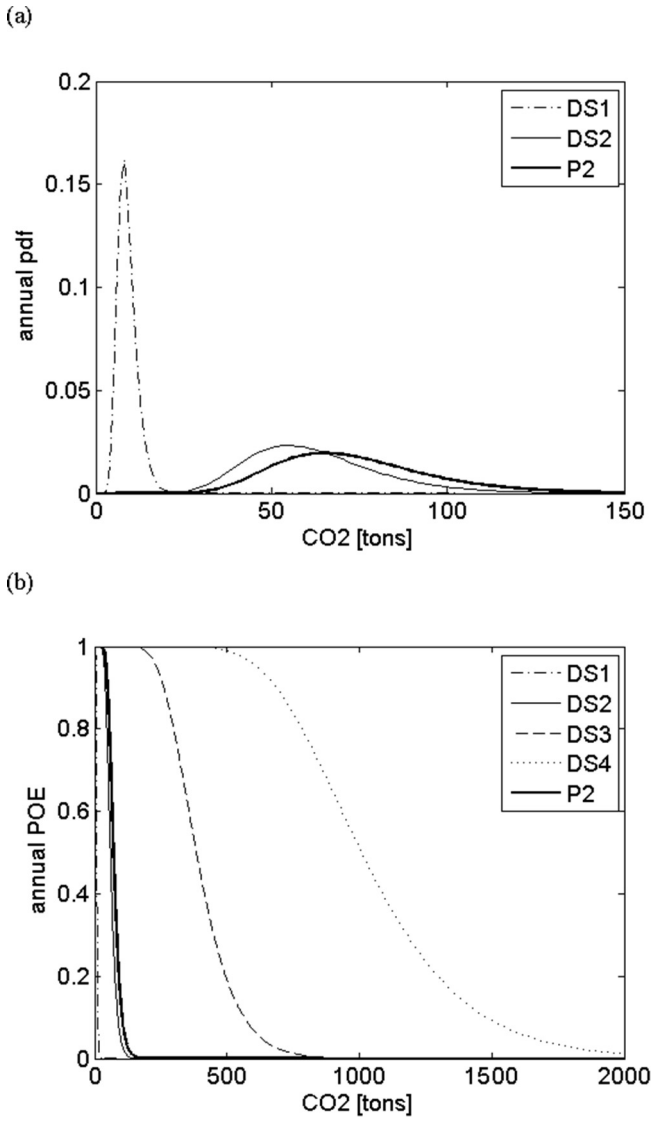

Fig. 11. POE of CO_2 emission given different damage states and energy plan.

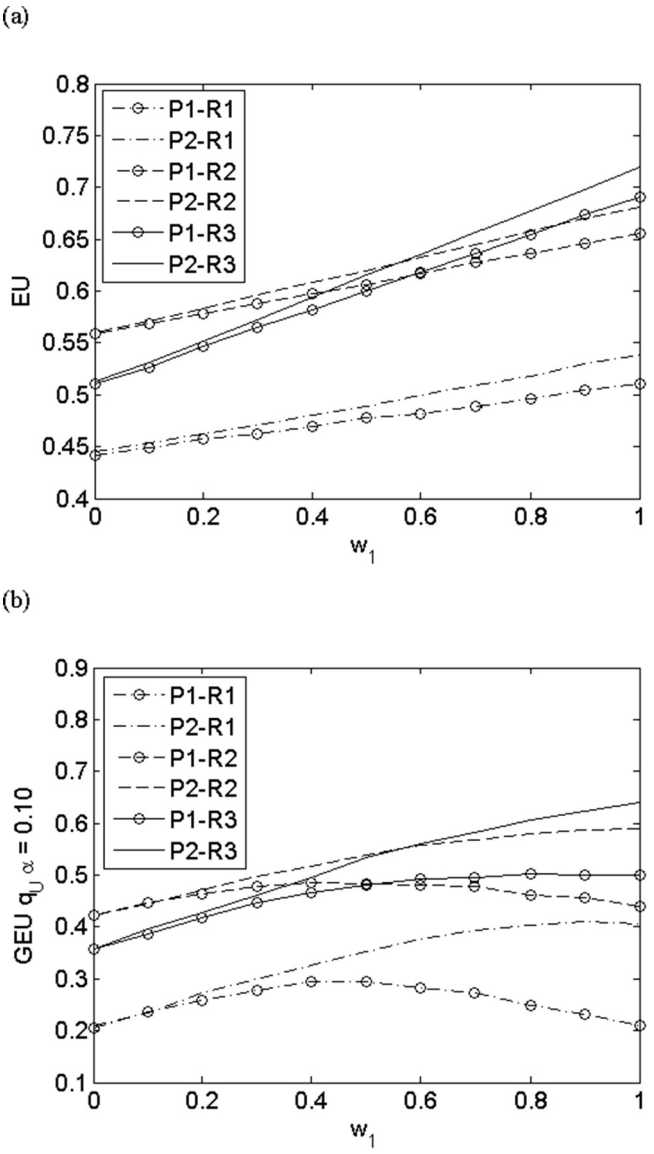

Fig. 12. Sensitivity analysis of the *GEU* in terms of the weight $w_1 \equiv w_{CO_2}$, (a) *EU*, (b) *GEU* measured through superquantile with $\alpha = 0.1$ for the holistic design.

cumulative prospect theory and it can incorporate, as particular cases, the expected utility and the expected cost. To quantify the risk perception inside the *GEU*, the superquantile applied to the utility has been proposed. This allows to take into account the risk-aversion of the decision maker towards the extreme events. The considered example building has also shown that the risk-averse "best" choice is typically different from an average alternative.

Quantiles and superquantiles of the utilities have been determined through the first-order reliability method (FORM), which offers some distinct advantages: (*i*) good efficiency in terms of computational cost, also in the range of the small probabilities, and (*ii*) the design point gives information about the most critical realizations of the performances. The latter advantage is of interest in a multi-criteria decision-making process, because a good knowledge of the consequences may support the decision maker in making rational choices.

The application to a hypothetical office building has shown the strengths of the proposed approach as a decision support tool under risk for holistic building design. The example has also shown that design by resilience may imply design by sustainability and that a "green" building design (alone) may not be resilient in the face of extreme events.

In the proposed numerical study some simplifying assumptions have been considered to underline some features of the approach, e.g. the repair costs of the non-structural components (architectural, mechanical and electrical) have not been included in the analysis, and the costs of construction of the buildings have been chosen to show that greater robustness may not imply necessarily the minimum total loss. Illustrative aims drove the choice of the case study. Future research will be devoted to the extension of the method in the framework of lifecycle analysis [18] applied to real engineering buildings. In that regard, several types of new design concepts and materials can be compared to determine the most sustainable site-dependent solution for each type of building.

Acknowledgements

This research was funded by the Republic of Singapore's National Research Foundation through a grant to the Berkeley Education Alliance for Research in Singapore (BEARS) for the Singapore Berkeley Building Efficiency and Sustainability in the Tropics (SinBerBEST) program. BEARS has been established by the University of California, Berkeley, USA, as a center for intellectual excellence in research and education in Singapore.

References

[1] UNISDR. Making Development Sustainable: The Future of Disaster Risk Management. Global Assessment Report on Disaster Risk Reduction. 2015. doi: 9789211320282.
[2] Bruneau M, Chang SE, Eguchi RT, Lee GC, O'Rourke TD, Reinhorn AM, et al. A framework to quantitatively assess and enhance the seismic resilience of communities. Earthq Spectra 2003;19:733–52. http://dx.doi.org/10.1193/1.1623497.
[3] NIST. Community Resilience Planning Guide. NIST 2015:4–5.
[4] Brundtland GH. Our Common Future: Report of the World Commission on Environment and Development. vol. 4. 1987. doi: 10.1080/07488008808408783.
[5] Keeney R, Raiffa H. Decisions with multiple objectives–preferences and value tradeoffs. vol. 39. 1993. doi:10.1002/bs.3830390206.
[6] Günay S, Mosalam KM. PEER performance-based earthquake engineering methodology. Revisited. J Earthq Eng 2013;17:829–58. http://dx.doi.org/10.1080/13632469.2013.787377.
[7] Benjamin JR, Cornell CA. Probabilit, Statistics and decision for civil enigneers. McGraw-Hill; 1970.
[8] Tversky A, Kahneman D. Judgment under uncertainty: heuristics and biases. Science (80-) 1974;185:1124–31. http://dx.doi.org/10.1126/science.185.4157.1124.
[9] Von Neumann J, Morgenstern O. Theory of games and economic behavior Princet Univ Press; 1944. http://dx.doi.org/10.1177/1468795X06065810. pp. 625.
[10] Allais M, Hagen O. Expected Utility Hypotheses and the Allais Paradox. 1979.
[11] Kahneman D, Tversky A. Prospect theory: an analysis of decision under risk. Econometrica 1979;47:263–92. http://dx.doi.org/10.2307/1914185.
[12] Tversky A, Kahneman D. Advances in prospect theory: cumulative representation of uncertainty. J Risk Uncertain 1992;5:297–323. http://dx.doi.org/10.1007/BF00122574.
[13] Cha EJ, Ellingwood BR. Seismic risk mitigation of building structures: the role of risk aversion. Struct Saf 2013;40:11–9. http://dx.doi.org/10.1016/j.strusafe.2012.06.004.
[14] Goda K, Hong HP. Application of cumulative prospect theory: implied seismic design preference. Struct Saf 2008;30:506–16. http://dx.doi.org/10.1016/j.strusafe.2007.09.007.
[15] Artzner P, Delbaen F, EBER Société Générale J, David Heath P. Coherent Measures of Risk. Math Financ 1999;9:203–28. doi: 10.1111/1467-9965.00068.
[16] Rockafellar RT, Royset JO. Engineering decisions under risk averseness. ASCE-ASME J Risk Uncertain Eng Syst Part A Civ Eng 2015;1:4015003. http://dx.doi.org/10.1061/AJRUA6.0000816.
[17] Maes MA, Faber MH. Utility, Preferences, and Risk Perception in Engineering Decision Making. 2008.
[18] Alibrandi U, Mosalam KM. A Decision Support Tool for Sustainable and Resilient Building Design. In: Gardoni P, editor. Risk Reliab. Anal. Theory Appl. –, Springer Series in Reliability Enigneering; 2017, p. 509–36.
[19] Konstantakopoulos I, Ratliff LJ, Jin M, Sastry SS, Spanos CJ. Robust utility learning with applications to Social Games in Smart Buildings. IEEE Trans. Control Syst. Technol. 2018.
[20] Konstantakopoulos I, Alibrandi U, Mosalam KM, Spanos CJ. Hierarchical decision making by leveraging utility theory and game theoretic analysis towards sustainability in building design operation. 6th Int. Symp. Reliab. Eng. Risk Manag. (6ISRERM), 2018.
[21] San-José Lombera J-T, Garrucho Aprea I. A system approach to the environmental analysis of industrial buildings. Build Environ 2010;45:673–83. http://dx.doi.org/10.1016/j.buildenv.2009.08.012.
[22] Pons O, Aguado A. Integrated value model for sustainable assessment applied to technologies used to build schools in Catalonia. Spain. Build Environ 2012;53:49–58. http://dx.doi.org/10.1016/j.buildenv.2012.01.007.
[23] Wang JJ, Jing YY, Zhang CF, Zhao JH. Review on multi-criteria decision analysis aid in sustainable energy decision-making. Renew Sustain Energy Rev 2009;13:2263–78. http://dx.doi.org/10.1016/j.rser.2009.06.021.
[24] Winston WL. Operations Research: Applications and Algorithms. 2003. doi:10.1007/SpringerReference_20294.
[25] Haukaas T. Probabilistic models, methods, and decisions in earthquake engineering. Safety, Reliab. Risk Life-Cycle Perform. Struct. Infrastructures – Proc. 11th Int. Conf. Struct. Saf. Reliab. ICOSSAR 2013, 2013, p. 47–66.
[26] Yang TY, Moehle J, Stojadinovic B, Der Kiureghian A. An application of PEER performance-based earthquake engineering methodology. 8th US Natl Conf Earthq Eng 2006:1–10.
[27] Ditlevsen O. Decision modeling and acceptance criteria. Struct Saf 2003;25:165–91. http://dx.doi.org/10.1016/S0167-4730(02)00048-6.
[28] Cha EJ, Ellingwood BR. Risk-averse decision-making for civil infrastructure exposed to low-probability, high-consequence events. Reliab Eng Syst Saf 2012;104:27–35. http://dx.doi.org/10.1016/j.ress.2012.04.002.
[29] Gardoni P, Guevara-Lopez F, Contento A. The life profitability method (LPM): a financial approach to engineering decisions. Struct Saf 2016;63:11–20.
[30] Yaari ME. The dual theory of choice under risk. Econometrica 1987;55:95. http://dx.doi.org/10.2307/1911158.
[31] Alibrandi Ma C, Koh CG. Secant hyperplane method for structural reliability analysis. J Eng Mech 2016;142:4015098.
[32] Alibrandi U, Mosalam KM. Equivalent linearization methods for nonlinear stochastic dynamic analysis using linear response surfaces. J Eng Mech 2017;143.
[33] Der Kiureghian A, Zhang Y, Li CC. Inverse Reliability problem. J Eng Mech 1994;120:1154–9.
[34] Cornell CA, Krawinkler H. Progress and challenges in seismic performance assessment. PEER Cent News 2000;3:1–4.
[35] Wei H, Shohet IM, Skibniewski M, Shapira S, Yao X. Assessing the lifecycle sustainability costs and benefits of seismic mitigations designs for buildings Title. J Archit Eng 2016:22.
[36] Nielsen TD, Jensen FV. Bayesian Network and Decision Graph. 2009. doi: 10.1007/978-0-387-68282-2.
[37] Jaynes ET. Information theory and statistical mechanics. Phys Rev 1957;106:181–218. http://dx.doi.org/10.1103/PhysRev. 106.620.
[38] Kapur J, Kesavan H. Entropy optimization principles with applications. San Diego, NY: Academic Press; 1992.
[39] Alibrandi U, Mosalam KM. The Kernel Density Maximum Entropy with Generalized Moments for evaluating probability distributions, including tails, from small sample of data. Int J Numer Methods Eng 2017. http://dx.doi.org/10.1002/nme.5725.
[40] Alibrandi U, Mosalam KM. Code-conforming PEER PBEE using stochastic dynamic analysis and information theory. KSCE J Civ Eng 2018;22:1002–15.
[41] Alibrandi U, Koh CG. First Order Reliability Method for structural reliability analysis in presence of random and interval variables. ASCE-ASME J Risk Uncertain Eng Syst Part B Mech Eng 2015;1.
[42] Ramamoorthy SK, Gardoni P, Bracci JM. Probabilistic demand models and fragility curves for reinforced concrete frames. J Struct Eng Asce 2006;132:1563–72. http://dx.doi.org/10.1061/(ASCE)0733-9445(2006) 132:10(1563).
[43] Wen YK, Kang YJ. Minimum life-cycle cost design criteria. Struct Saf Reliab 1998;1–3:1047–54.
[44] Field EH, Jordan TH, Cornell CA. OpenSHA: a developing community-modelling environment for seismic hazard analysis. Seismol Res Lett 2003;74:406–19.
[45] PEER. PEER NGA Ground Motion Database. 2011.
[46] McKenna F. Opensees Useer's Manual. 2010.
[47] FEMA. Earthquake model HAZUS, MH Technical Manual. Washington DC: 2013.
[48] Wen YK, Ellingwood BR, Bracci J. Vulnerability function framework for consequence-based engineering. Mid-America Earthq Cent Proj 2004:1–101.
[49] Williams RJ, Gardoni P, Bracci JM. Decision analysis for seismic retrofit of structures. Struct Saf 2009;31:188–96. http://dx.doi.org/10.1016/j.strusafe.2008.06.017.
[50] Doe/Eia. Annual Energy Review 2011. 2012. doi:/EIA-1384(2011).
[51] Us Epa. US Environmental Protection Agency. US Environ Prot Agency 2012.